Catal Lett (2008) 126:313–318
DOI 10.1007/s10562-008-9621-3

Effect of Support Crystallite Size on Catalytic Activity and Deactivation of Nanocrystalline $ZnAl_2O_4$-Supported Pd Catalysts in Liquid-Phase Hydrogenation

Terachai Sirikajorn · Okorn Mekasuwandumrong · Piyasan Praserthdam · James G. Goodwin Jr. · Joongjai Panpranot

Received: 21 November 2007 / Accepted: 28 March 2008 / Published online: 9 September 2008

Abstract The catalytic activity and deactivation of nanocrystalline $ZnAl_2O_4$-supported Pd catalysts were investigated for the liquid-phase hydrogenation under mild conditions. Nanocrystalline $ZnAl_2O_4$ spinels with average crystallite size between 8 and 33 nm were synthesized by the solvothermal method in toluene. Higher turnover frequencies for 1-heptyne hydrogenation and less deactivation due to Pd leaching were obtained for the Pd/$ZnAl_2O_4$-33 nm catalyst. XPS and ESR results suggest that the presence of defects in larger crystallite size $ZnAl_2O_4$ resulted in higher Pd dispersion and stronger interaction between Pd and the support.

Keywords $ZnAl_2O_4$ spinel · Solvothermal · Nanocrystals · Pd catalyst · Liquid-phase hydrogenation · 1-heptyne hydrogenation

1 Introduction

Supported Pd catalysts are widely used in liquid-phase selective alkyne hydrogenation especially for the synthesis of fine chemicals and bio-active compounds [1–4]. The notable advantages of supported noble metal catalysts under heterogeneous conditions are relatively high activity, mild process conditions, easy separation, and better handling properties. The commonly used supports for Pd catalysts include activated carbon [5, 6], silica [7], alumina [8], and to a lesser extent, polymer [9] and zeolite [10]. It is known that the choice of an efficient support can significantly improve the activity, selectivity, recycling, and reproducibility of Pd catalyst systems [11–13]. Recently, spinel type oxides like $ZnAl_2O_4$ have been used as supports for Pt and Pd catalysts and a distinct metal-support interaction was found [14, 15]. It has also been reported that Rh complexes were effectively and stably bound to hydrothermally synthesized $ZnAl_2O_4$ better than to Al_2O_3 [16].

The solvothermal method is one of the most interesting methods for preparation of nanocrystalline materials. It has been used to successfully synthesize various types of nanosized metal oxides with large surface areas, high crystallinities, and high thermal stabilities [17, 18]. The products obtained by solvothermal synthesis usually show uniform morphology, well-controlled chemical composition, and narrow particle size distribution. As catalyst supports, solvothermal-derived nanocrystalline oxides have been shown to provide better catalytic properties of the corresponding supported metal catalysts compared to commercially available supports [19–21]. In this study, nanocrystalline $ZnAl_2O_4$ spinels were prepared by the solvothermal method using toluene as the solvent and were employed as Pd catalyst supports. The effect of support crystallite size in the range of 8–33 nm on the catalytic

---

T. Sirikajorn · P. Praserthdam · J. Panpranot (✉)
Center of Excellence on Catalysis and Catalytic Reaction Engineering, Department of Chemical Engineering, Faculty of Engineering, Chulalongkorn University, Bangkok 10330, Thailand
e-mail: joongjai.p@eng.chula.ac.th

O. Mekasuwandumrong
Department of Chemical Engineering, Silpakorn University, Sanam Chandra Palace Campus, Nakorn Pathom 73000, Thailand

J. G. Goodwin Jr.
Department of Chemical and Biomolecular Engineering, Clemson University, Clemson, SC 29634, USA

activities, selectivities, and catalyst deactivation due to metal leaching of the nanocrystalline $ZnAl_2O_4$-supported Pd catalysts were investigated by X-ray diffraction (XRD), N_2 physisorption, transmission electron microscopy with selected area electron diffraction (TEM with SAED), CO pulse chemisorption, electron spin resonance (ESR), X-ray photoelectron spectroscopy (XPS), and atomic absorption spectroscopy (AAS). Liquid-phase hydrogenation of 1-heptyne under mild reaction conditions was used as a test reaction.

2 Experimental

2.1 Preparation of $ZnAl_2O_4$ and Pd/$ZnAl_2O_4$

Zinc aluminate spinel ($ZnAl_2O_4$) was prepared by the solvothermal technique using aluminium isopropoxide (Aldrich) and zinc (II) acetylacetonate (Merck) (Zn/Al molar ratio = 0.5) as reactants suspended in toluene (Carlo Erba Reagenti). First, the mixture of aluminium isopropoxide, 15.0 g and appropriate amount of zinc (II) acetylacetonate (Zn/Al molar ratio = 0.5) was prepared in 100 cm^3 toluene in a 1.5-dm^3 autoclave reactor. The suspension was heated to 300 °C at the rate of 2.5 °C/min and held at that temperature for 2 h. The resulting products were washed with methanol and dried in air and then calcined in a furnace at various temperatures (500, 700, 900, or 1,150 °C) for 1 h. The as-synthesized $ZnAl_2O_4$ was referred to as $ZnAl_2O_4$-as-syn and the calcined $ZnAl_2O_4$ supports were denoted as $ZnAl_2O_4$-500, $ZnAl_2O_4$-700, $ZnAl_2O_4$-900, $ZnAl_2O_4$-1150 according to the calcination temperature used.

Pd/$ZnAl_2O_4$ catalysts were prepared by the incipient wetness impregnation method using $Pd(NO_3)_2$ (Aldrich) as the palladium precursor. The support was impregnated to incipient wetness with an aqueous solution containing sufficient palladium to result in 1 wt% Pd catalysts. The catalyst samples were dried in an oven at 100 °C overnight and calcined in air at 400 °C for 6 h prior to characterization.

2.2 Catalyst Characterization

The specific surface areas, pore volumes, and average pore diameters were determined by N_2 physisorption using a Micromeritics ASAP 2000 automated system and the Brunauer-Emmet-Teller (BET) method. Each sample was degassed under vacuum at <10 μm Hg in the Micromeritics system at 150 °C for 4 h prior to N_2 physisorption. The XRD patterns of the catalysts were measured from 10° to 80° 2θ using a SIEMENS D5000 X-ray diffractometer and Cu K_α radiation with a Ni filter. Catalyst crystallite sizes and diffraction patterns of supports were obtained using the JEOL JEM 2010 transmission electron microscope that employed a LaB_6 electron gun in the voltage range of 80–200 kV with an optical point-to-point resolution of 0.23 nm. The amounts of CO chemisorbed on the catalysts were measured at room temperature using a Micromeritic Chemisorb 2750 automated system with ChemiSoft TPx software. Prior to chemisorption, the sample was reduced in a H_2 flow at 500 °C for 2 h and then cooled down to ambient temperature in a He flow. The bulk compositions of palladium in the catalysts before and after reaction were determined using a Varian Spectra A800 atomic absorption spectrometer. Electron spin resonance spectroscopy (ESR) was conducted using a JEOL JESRE2X-electron spin resonance spectrometer. The intensity of ESR was calculated using a computer software program ES-PRIT ESR DATA SYSTEM (version 1.6).

2.3 Reaction Study

Liquid-phase partial hydrogenation of 1-heptyne was carried out in a 50-cm^3 stainless steel autoclave. Approximately 0.02 g of supported Pd catalyst was placed in the reactor with 10 cm^3 of 2 vol% of 1-heptyne in toluene. Afterward the reactor was filled with hydrogen at 1 bar pressure. Stirring was switched on to start the reaction, and reaction was carried out for 5 min. The products were analyzed by gas chromatography with a flame ionization detector.

3 Results and Discussion

3.1 Catalyst Characteristics

Figure 1 shows the XRD patterns of the as-synthesized and calcined $ZnAl_2O_4$ powders. Reaction of the mixture of aluminum isopropoxide (AIP) and zinc acetylacetonate (ZnAcAc) in toluene yielded the nanocrystalline spinel $ZnAl_2O_4$ powders with no other impurities. Increasing calcination temperature resulted in a subsequent increase in the degree of crystallinity and in the crystallite size. The average crystallite size of $ZnAl_2O_4$ powders calculated from the Scherrer equation was found to increase linearly from 8 to 33 nm with increasing calcination temperature to 1,150 °C. The average crystallite sizes, BET surface areas, pore volumes, and average pore diameters of the solvothermal-derived $ZnAl_2O_4$ are given in Table 1. The BET surface areas gradually decreased with increasing calcination temperature suggesting that sintering occurred during the calcination process corresponding to the increase of crystallite size. The pore size distributions of the $ZnAl_2O_4$ supports are shown in Fig. 2. It was found that the calcined

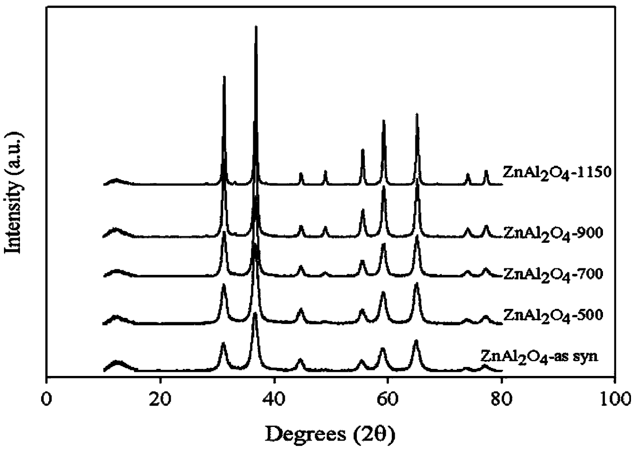

Fig. 1 XRD patterns of the as-synthesized and the calcined $ZnAl_2O_4$

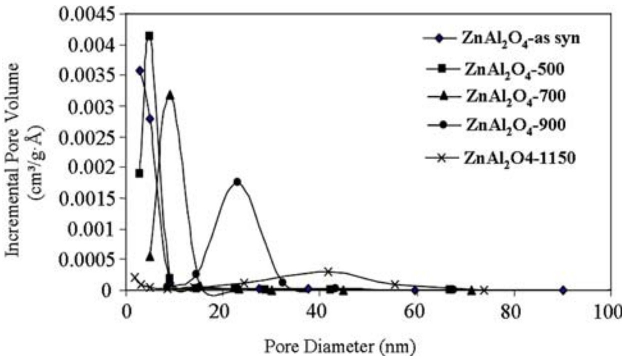

Fig. 2 Pore size distribution of the as-synthesized and the calcined $ZnAl_2O_4$

$ZnAl_2O_4$ samples retained their large pore volume and narrow pore size distribution during high temperature calcination up to 700 °C. Significant loss of pore volume was found for the sample calcined at 1,150 °C ($ZnAl_2O_4$-33 nm).

Figure 3 shows the transmission electron micrographs with selective area electron diffraction (SAED) pattern of various $ZnAl_2O_4$ spinels. The crystallites of $ZnAl_2O_4$ consisted of particles which were agglomerates of smaller crystallites with primarily spherical shapes. The average crystal sizes of the as-prepared and the calcined samples determined from TEM were similar to those measured from the XRD line broadening. The corresponding selected area diffraction patterns confirmed the structure of $ZnAl_2O_4$ and there was no significantly difference in SAED patterns of the as-synthesized and the calcined samples (not shown), indicating that all the samples contained only crystalline $ZnAl_2O_4$.

The presence of defect sites on the nanocrystalline supports was detected using electron spin resonance spectrometry. ESR is known as an effective method for investigating of the electron spin state and the structure of the surface of nano-sized crystallites. The ESR signals from the various solvothermal-derived nanocrystalline $ZnAl_2O_4$ are shown in Fig. 4. It is shown that only the $ZnAl_2O_4$-33 nm sample exhibited very strong and stable ESR signals. These ESR signals may arise from O^{2-} vacancies on the surface and/or incorporation of trace impurities in their crystal structure during high temperature calcination resulting in crystal distortion. Moreover, it has been reported that nano-sized $ZnAl_2O_4$ possesses inverse structure when calcined at temperatures <900 °C [22]. The highly crystalline nature (regular spinel structure) of $ZnAl_2O_4$ was obtained at calcination temperatures ≥1,000 °C. The result in this study, however, was in agreement with literature that larger crystallites of nanocrystalline materials synthesized by the solvothermal method contain more defects than smaller ones [23].

3.2 Characteristics and Catalytic Properties of Nanocrystalline $ZnAl_2O_4$-Supported Pd Catalysts

The physicochemical properties of Pd supported on as-synthesize and calcined nanocrystalline $ZnAl_2O_4$ are shown in Table 2. For the as-synthesized ones, the BET surface areas were slightly decreased after impregnation with Pd suggesting pore blockage by Pd/PdO clusters. However, for the calcined $ZnAl_2O_4$ supportd ones, there were less differences in BET surface areas of the supports and of the supported Pd catalysts suggesting that much of the Pd/PdO may have been located on the external surfaces. The relative amounts of active surface Pd metal atoms on the catalyst samples were calculated from CO chemisorption experiments at room temperature. The calculation of Pd active sites was based on the assumption that

Table 1 N_2 physisorption results[a] and XRD determined average crystallite sizes of the as-synthesized and the calcined $ZnAl_2O_4$ supports prepared by the solvothermal method

Sample	BET S.A. (m^2/g)	Pore volume (m^3/g)	Avg. pore diameter (nm)	Avg. XRD crystallite size (nm)
$ZnAl_2O_4$-as-syn	130	0.18	4.2	8.2
$ZnAl_2O_4$-500	116	0.19	4.6	9.0
$ZnAl_2O_4$-700	63	0.20	8.5	10.9
$ZnAl_2O_4$-900	28	0.19	22.0	17.6
$ZnAl_2O_4$-1150	15	0.08	36.6	33.3

[a] Error of measurements as determined directly were ±10%

Fig. 3 TEM micrographs and selected area electron diffraction of various $ZnAl_2O_4$ samples

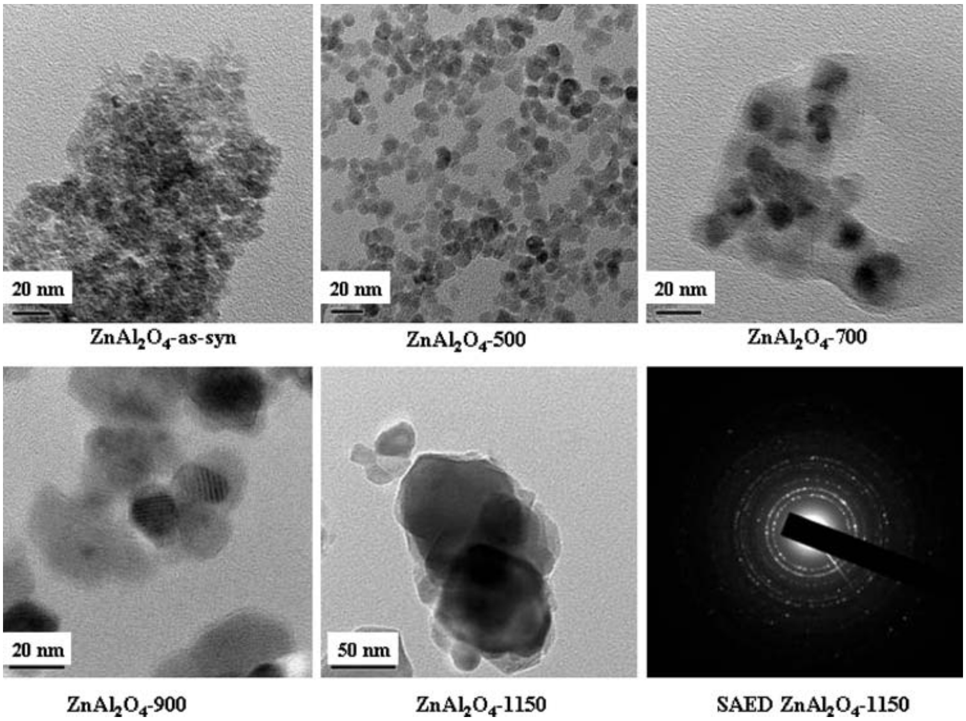

$ZnAl_2O_4$-as-syn $ZnAl_2O_4$-500 $ZnAl_2O_4$-700

$ZnAl_2O_4$-900 $ZnAl_2O_4$-1150 SAED $ZnAl_2O_4$-1150

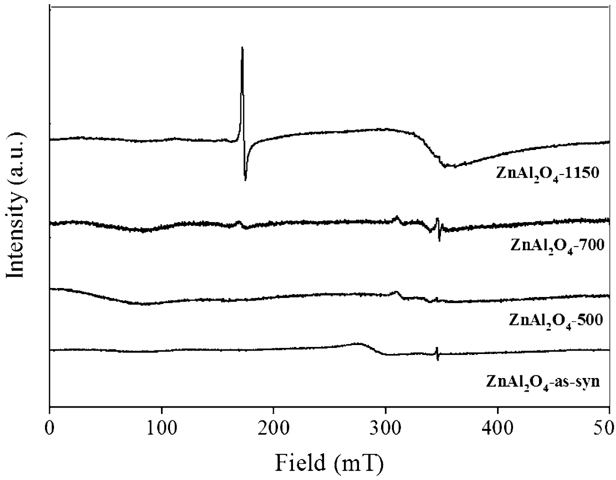

Fig. 4 ESR results of the solvothermal-derived $ZnAl_2O_4$

one carbon monoxide molecule adsorbs on one palladium surface atom or site [24]. It is surprising that the amounts of CO chemisorption were essentially similar for the Pd catalysts supported on $ZnAl_2O_4$ with the average crystallite sizes in the range of 8–18 nm. The amount of CO chemisorption was increased for the one supported on $ZnAl_2O_4$-33 nm. The percentages of Pd dispersion and corresponding Pd^0 particle sizes were calculated based on the CO chemisorption results and are also given in Table 2.

The catalytic properties of all the catalyst samples were investigated for the liquid-phase hydrogenation of 1-heptyne under mild conditions using a stirred batch reactor. The results are summarized in Table 3. The conversions of 1-heptyne for various Pd/$ZnAl_2O_4$ catalysts were in the range of 45–66% with Pd/$ZnAl_2O_4$-33 nm exhibiting the highest conversion. There were no appreciable influences on 1-heptene selectivity since all the catalysts exhibited high selectivities for 1-heptene (97–100%). The specific activities of the Pd/$ZnAl_2O_4$ catalysts are also expressed in terms of turnover frequency (TOF) which is defined as mole of product/mole of surface metal atoms/time. This is not a perfect measure of TOF since it is for reaction with a high conversion and therefore affected by changing reactant concentration. However, it is given here as a rough comparison of specific rate.

The actual amounts of palladium loading before and after reaction were determined by atomic adsorption spectroscopy and the %Pd leached for each catalyst is given in Table 3. Before reaction, palladium loading on all the catalyst samples was approximately 1.2 wt%. After one batch reaction period, the amount of palladium loading decreased to 0.6–1.1 wt% indicating that leaching of palladium occurred during reaction for most of the catalysts. Leaching of the active metal is one of the main causes of catalyst deactivation in liquid phase reactions. It depends upon the reaction medium (pH, oxidation potential, chelating properties of molecules) and upon bulk and surface properties of the metal [25]. The percentages of palladium leaching were found to be much lower when Pd catalysts were supported on $ZnAl_2$O4-33 nm compared to those on smaller crystallite size ones.

Table 2 Physicochemical properties of the various Pd catalysts

Catalysts	BET S.A.[a] (m^2/g)	Pore volume[a] (m^3/g)	Avg. pore diameter[a] (nm)	CO chemisorption[b] (10^{18} molecules CO/g cat.)	Dispersion(%)[c]	Pd^0 d_P[d] (nm)
$Pd/ZnAl_2O_4$-as-syn	106	0.20	4.6	7.4	13.0	7.8
$Pd/ZnAl_2O_4$-500	104	0.21	4.8	7.4	13.1	7.8
$Pd/ZnAl_2O_4$-700	66	0.21	8.9	7.2	12.8	7.4
$Pd/ZnAl_2O_4$-900	28	0.18	21.5	7.3	12.8	8.0
$Pd/ZnAl_2O_4$-1150	16	0.10	29.2	8.7	15.3	6.7

[a] Determined from N_2 physisorption. Error of measurements as determined directly were ±10%

[b] Error of measurements for CO chemisorption as determined directly were ±5%

[c] Based on total palladium loading and an assumption of CO/Pd = 1

[d] Based on $d = (1.12/D)$ nm [24], where D = fractional metal dispersion

Table 3 Catalytic properties for liquid-phase 1-heptyne hydrogenation[a]

Catalysts	Conversion of 1-heptyne (%)	1-Heptene selectivity (%)	Estimated TOF[b] (s^{-1})[c]	%Pd leached[d]
$Pd/ZnAl_2O_4$-as-syn	52	97	0.24	36
$Pd/ZnAl_2O_4$-500	51	100	0.23	38
$Pd/ZnAl_2O_4$-700	45	100	0.22	30
$Pd/ZnAl_2O_4$-900	49	100	0.24	35
$Pd/ZnAl_2O_4$-1150	66	100	0.32	6

[a] Reaction conditions were 105 kPa, 30 °C, 5 min, and catalyst/substrate molar ratio = 1,600

[b] TOF = mole product/mole Pd metal surface atoms/s. Based on the amount of potentially active Pd atoms measured by CO chemisorption

[c] Estimated since at high conversion

[d] Based on atomic absorption spectroscopy results. Error of measurement as determined directly was ±10%

The mechanism of metal leaching usually involves metal compounds that are formed and are soluble in the reaction mixture. However, it is unlikely that 1-heptyne forms a compound with Pd at room temperature, unless it is some hydrido-organic complex. It is likely that Pd was leached in the form of Pd hydride phase. Under certain conditions, Pd-β-hydride can appear as a soft material with higher mechanical abrasion [26]. Moreover, leaching of Pd may depend on Pd particle size, larger particles are more likely to be leached since larger particles formed Pd-β-hydride more easily [27, 28]. Similar results have been reported previously by our group for the deactivation of Pd/SiO_2 catalysts during liquid-phase hydrogenation [29, 30]. The leached Pd species, however, appeared to be inactive for the present hydrogenation since the catalyst recycling test showed minimal loss of activity after it was reused for several cycles. Moreover, Pd-β-hydride is expected to have a different catalytic activity from that of metallic palladium [31].

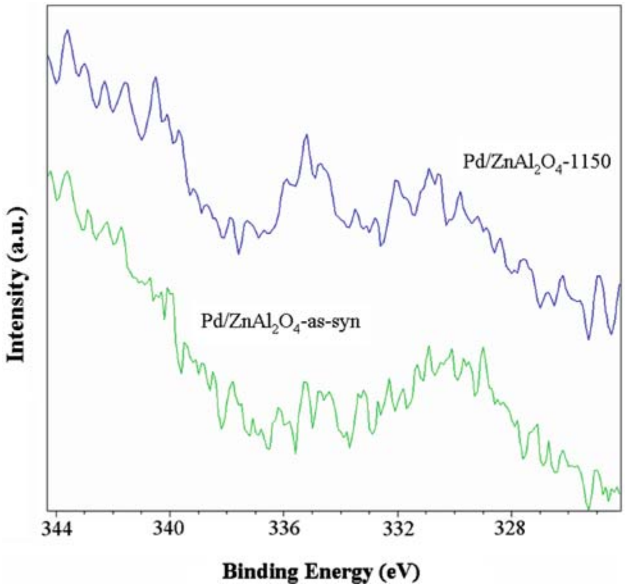

Fig. 5 XPS spectra of Pd $3d_{5/2}$ for $Pd/ZnAl_2O_4$ catalysts

The interaction between Pd and the nanocrystalline supports was also studied by XPS analysis, the Pd $3d_{5/2}$ core level binding energy of the various catalyst samples are shown in Fig. 5. It can be seen that the Pd $3d_{5/2}$ binding energy for Pd catalyst supported on the $ZnAl_2O_4$-33 nm shifted towards higher binding energy suggesting a stronger interaction between Pd and the highly crystalline supports. Among the various $ZnAl_2O_4$ samples in this

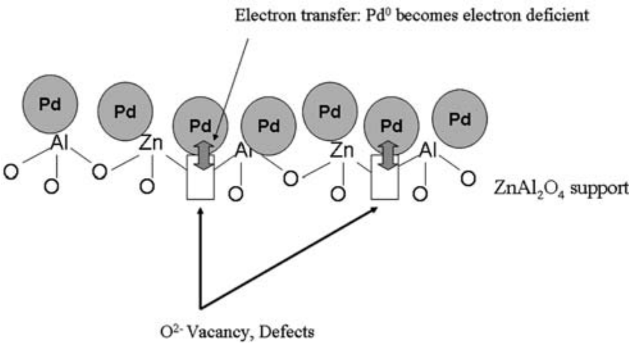

Fig. 6 A conceptual model for stronger metal-support interaction induced by defect sites of the nanocrystalline material

study, only the $ZnAl_2O_4$-33 nm possessed significant amount of defects. Thus, it is hypothesized that electron transfer occurred at the defective points of the nanocrystalline materials from Pd to the support, and, as a consequence, Pd^0 surface atoms became electron deficient and their catalytic properties were modified. A conceptual model for stronger metal-support interaction induced by defective sites of $ZnAl_2O_4$-33 nm is illustrated in Fig. 6.

4 Conclusions

The catalytic activities and deactivation of Pd catalysts supported on the solvothermal-derived nanocrystalline $ZnAl_2O_4$ in liquid-phase hydrogenation of 1-heptyne were investigated. Higher turnover frequencies and less Pd leaching were obtained on the Pd catalyst supported on larger crystallite size $ZnAl_2O_4$ that contained significant amounts of defects (as shown by strong and stable ESR signals). It is suggested that the presence of defects on these nanocrystalline materials induced stronger metal-support interaction between Pd and the supports thus their catalytic properties were modified.

Acknowledgments Financial supports from the Thailand Research Fund (RMU50-Joongjai Panpranot), the Graduate School of Chulalongkorn University (the 90th Anniversary of Chulalongkorn University-the Golden Jubilee Fund), and the Commission on Higher Education, Ministry of Education, Thailand are gratefully acknowledged.

References

1. Guczi L, Horvath A, Beck A, Sarkany A (2003) Stud Surf Sci Catal 145:351
2. Dominguez-Quintero O, Martinez S, Henriquez Y, D'Ornelas L, Krentzien H, Osuna J (2003) J Mol Catal A 197:185
3. Stanger KJ, Tang Y, Anderegg J, Angelici RJ (2003) J Mol Catal A 202:147
4. Nijhuis TA, van Koten G, Moulijn JA (2003) Appl Catal A 238:259
5. Chou P, Vannice MA (1987) J Catal 107:129
6. Jackson SD, Shaw LA (1996) Appl Catal A 134:91
7. Cherkashin GM, Shuikina LP, Parengo OP, Frilov VM (1985) Kinet Katal 26:1110
8. L'Argentiere PL, Liprandi DA, Cagnola EA, Figoli NS (1997) Catal Lett 44:101
9. Mathew JP, Srinivasan M (1995) Eur Polym J 31:835
10. Choudary BM, Kantam ML, Reddy NM, Rao KK, Haritha Y, Bhaskar V, Figueras F, Tuel A (1999) Appl Catal A 181:139
11. Shen WJ, Okumura M, Matsumura Y, Haruta M (2001) Appl Catal A 213:225
12. Pinna F, Menegazzo F, Signoretto M, Canton P, Fagherazzi G, Pernicone N (2001) Appl Catal A 219:195
13. Panpranot J, Pattamakomson K, Praserthdam P, Goodwin JG Jr (2004) Ind Eng Chem Res 43:6014
14. Wrzyszcz J, Zawadzki M, Trawczynski J, Grabowska H, Mista W (2001) Appl Catal A 210:263
15. Zawadzki M, Mista W, Kepinski L (2001) Vacuum 63:291
16. Wrzyszcz J, Zawadzki M, Trzeciak AM, Ziolkowski JJ (2002) J Mol Catal A 189:203
17. Inoue M, Kondo Y, Inui T (1988) Inorg Chem 27:215
18. Inoue M, Kominami H, Inui T (1992) J Am Ceram Soc 75:2597
19. Panpranot J, Taochaiyaphoom N, Praserthdam P (2005) Mater Chem Phys 94:207
20. Panpranot J, Nakkararuang L, Ngamsom B, Praserthdam P (2005) Catal Lett 103:53
21. Panpranot J, Taochaiyaphum N, Jongsomjit B, Praserthdam P (2006) Catal Commun 7:192
22. Mathur S, Veith M, Haas M, Shen H, Lecerf N, Huch V, Hufner S, Haberkorn R, Beck HP, Jilavi M (2001) J Am Ceram Soc 84:1921
23. Kongsuebchart W, Praserthdam P, Panpranot J, Sirisuk A, Supphasrirongjaroen P, Satayaprasert C (2006) J Crystal Growth 297:234
24. Mahata N, Vishwanathan V (2000) J Catal 196:262
25. Besson M, Gallezot P (2003) Catal Today 81:547
26. Albers P, Pietsch J, Parker SF (2001) J Mol Catal A 173:275
27. Shen WJ, Okumura M, Matsumura Y, Haruta M (2001) Appl Catal A 213:225
28. Neri G, Musolino MG, Milone C, Pietropaolo D, Glavagno S (2001) Appl Catal A 208:307
29. Panpranot J, Tangjitwattakarn O, Praserthdam P, Goodwin JG Jr (2005) Appl. Catal 292:322
30. Panpranot J, Pattamakomson K, Praserthdam P, Goodwin JG Jr (2004) Ind Eng Chem Res 43:6014
31. Walter J, Heiermann J, Dyker G, Hara S, Shioyama H (2000) J Catal 189:449